



ORIGINAL RESEARCH ARTICLE

Radiogallium-labeled gadolinium-porphyrin complex: A new agent for imaging and photodynamic therapy

Ali Arjmandpour^{1,2}, Yousef Fazaeli¹, Seyed Mohammad Mahdi Abtahi², Parviz Ashtari¹, Saeed Karampour¹, Gholamreza Shahhosseini¹, Shahzad Feizi¹

¹Radiation Application Research School, Nuclear Science and Technology Research Institute, Karaj, Iran

²Physics Department, Faculty of Basic Sciences, Imam Khomeini International University, Qazvin, Iran

ARTICLE INFO

Article History:

Received: 25 April 2022

Revised: 16 August 2022

Accepted: 23 August 2022

Published Online: 11 October 2022

Keyword:

Metalloporphyrin

Radiogallium

Gadolinium-porphyrin complex

Theranostic

*Corresponding Author:

Yousef Fazaeli

Address: Radiation Application Research School, Nuclear Science and Technology Research Institute (NSTRI), Moazzen Blvd., Rajaeeshahr, P.O. Box 31485-498, Karaj, Iran

Email: yfazaeli@aeoi.org.ir

ABSTRACT

Introduction: Metalloporphyrin-based contrast agents can improve probe functionality such as biocompatibility, prolonging presence in blood, and specific tumor accumulation. Herein, we report synthesis, structural characteristics, quality control, and nuclear imaging of new metalloporphyrin-based contrast agents.

Methods: To combine photodynamic therapy (PDT), magnetic resonance imaging (MRI), positron emission tomography (PET), and single-photon emission computerized tomography (SPECT), Gadolinium-proto porphyrin IX complex was synthesized via direct complexation method, then the metalloporphyrin (MP) was labeled with gallium-67 and gallium-68 in separated runs. *In-vivo* biodistribution studies were performed in mice bearing breast tumor (4T1 mouse mammary tumor cell line) and normal rats (for better visualization).

Results: Adsorption of the labeled compound into the tumor (ID/g % up to 4.6%), despite the small size of the tumor, had an upward trend at all times, and high and fast (less than 45 min) uptake of radiotracer in cancerous tumors was observed.

Conclusion: Fast and high tumor uptake revealed that this radiotracer could potentially be used as a theranostic agent.

Use your device to scan and read the article online



How to cite this article: Arjmandpour A, Fazaeli Y, Abtahi SMH, Ashtari P, Karampour S, Shahhosseini G, Feizi S. Radiogallium-labeled gadolinium-porphyrin complex: A new agent for imaging and photodynamic therapy. Iran J Nucl Med. 2023;31(1):35-41.

 <https://doi.org/10.22034/IRJNM.2022.40037>

INTRODUCTION

Recently, there has been growing interest in the development of tumor-specific diagnostic/therapeutic substances based on metalloporphyrin complexes to identify and destroy malignant and neoplastic tissue [1-5]. To improve theranostic efficacy in nuclear medicine, an ideal theranostic agent (ThA) should have biocompatibility, specificity, high tumor accumulation and fast excretion from body to minimize unwanted radiations. The first requirement for an efficient ThA is a high biocompatibility. Protoporphyrin IX (PpIX) is a biocompatible compound which is commonly used in PDT and has low cytotoxicity to human kidney cells and keratinocytes [6, 7]. The second factor is the rate of accumulation in tumor and ability to destroy cancer cells. PDT agents can accumulate preferentially in abnormal/malignant tissues. These tissues are subjected to the light source for generating cytotoxic reactive oxygen species which produce necrosis and/or apoptosis in them [8]. The ability to form stable complexes is the other critical factor to have a non-toxic agent. Due to the accumulation of metal ions in vital organs such as liver, kidney and bone marrow, gadolinium (Gd^{+3}) and gallium (Ga^{+3}) cannot be used as tracers in their ionic forms. This challenge can be addressed by complexation with porphyrins. Bohle et al.'s findings proposed a stable dimeric propionate-bridged dimer for Gallium (III) protoporphyrin IX [9, 10]. This structure was also confirmed by spectroscopic and theoretical experiments in another study [11].

Ga (III)-protoporphyrin IX chloride, can be taken up by *Staphylococcus aureus* within seconds and can be used for the treatment of drug-resistant staphylococcal infections [7]. Ga (III)-protoporphyrin IX at concentrations below 128 μ M does not show cytotoxicity on several human cell lines [12]. This complex did not change the behavior and health of mice after administration of one dose of 25-30 mg/kg followed by 4 daily dose of 10-12 mg/kg [13], but showed great antibacterial activity [14].

The progress in theranostic agents' development has bolstered the prospects of cancer detection and treatment through the evolution of a variety of hybrid compounds, which includes radiolabeled MRI agents with therapeutic properties [15]. Water soluble gadolinium porphyrin complexes were developed as multifunctional theranostic agents based on PDT, MRI, and phosphorescence-based oxygen indication [16, 17]. On the other hand, radiolabeled porphyrins were used successfully for detection and treatment of neoplastic lesions [18-26].

Photodynamic therapy is a noninvasive method for cancer therapy based on a photosensitizers (which are cyclic tetrapyrrolic scaffolds like porphyrins), light, and oxygen interaction. Usually, porphyrin molecules, which are accumulated in tumor cells, are excited by light to a triplet state and toxic reactive oxygen species (ROS) are generated. Protoporphyrin-IX and its metallic complexes have been used as photosensitizer for treatment of cancer [27-30]. Besides the anticancer applications, researchers proposed Protoporphyrin-IX and PDT as antimicrobial treatment. Fast improvement of drug design, pre-clinical and clinical trials, relative spread and increasing affordability of current medical approaches focus attention of scientist on easy adjustable theranostics, especially molecules with potential multimodal application to collect completely different information by using a single dose of medicine.

Due to the great potential of protoporphyrin IX for oncological imaging and treatment of tumors in PDT, it is of great interest to evaluate the biodistribution, tumor avidity, and the ability to form radiolabeled complexes while attaching to Gd^{+3} to form hetro-metal complex with ^{67}Ga and ^{68}Ga radionuclides. So, in this study, Gadolinium-protoporphyrin IX complex was synthesized, then the metalloporphyrin (MP) was labeled with gallium-67 and gallium-68. *In-vivo* biodistribution studies were studied in mice bearing breast tumor. The final products can be used as imaging agents using MRI, SPECT/ PET while they can also be used as PDT agent.

METHODS

Preparation of Gd (III)-protoporphyrin IX complex (PP IX-Gd)

All chemicals were obtained from Merck KGaA (Germany) and gallium radionuclides were provided from the Pars Isotope Company (Iran) (the activity of each Ga -68 generator was 40 mCi and Ga -67 was obtained in chloride form with the activity of 30 mCi in a volume of 0.5 ml). A mixture of 1 millimole of protoporphyrin IX disodium salt (3, 7, 12, 17-tetramethyl-8, 13-divinyl-2, 18-porphine dipropionic acid disodium salt, 606 mg) and 1 millimole of $GdCl_3$ (263 mg, 99.99%) in aqueous solvent (H_2O , 5ml) in the Ar atmosphere was allowed to be refluxed overnight in dark.

Radiolabeling of PP IX-Gd with gallium-67/68, quality control and animal studies

Typically, to label the protoporphyrin IX-gadolinium complex with gallium-67 and gallium-68 (in separate runs), 30 mCi of radionuclide in the form of $GaCl_3$, was dried using heat and passing nitrogen to remove

the HCl content. Then, 50 μ l of PP IX-Gd (from a 1mg/ml stock solution) and 1/5 ml of sodium acetate buffer (pH 5.5-6) were added and refluxed for 60 minutes. The final product was then passed through a 0.22 μ m filter and its pH was reset using the sodium acetate buffer in the range of 5.5-6.

Quality control

Radio thin layer chromatography (RTLC) was used to determine the radiochemical purity of the labeled porphyrin complex. A 5 μ l sample of the final product was fixed on Whatman No. 2 paper and placed in a RTLC tank containing 0.1 mM DTPA as mobile phase. After complete migration (10 cm) of the mobile phase, Whatman paper was removed from the tank and dried. It was then evaluated by the Bioscan AR-2000 RTLC scanner. Partition coefficient ($\log P$) of labeled compound was calculated followed by the determination of P (P =the ratio of specific activities of the 1-octanol and normal saline phases) [31].

Animal studies

3.7 MBq of the labeled compounds were injected to rodents via tail vein with insulin syringes. SPECT and PET (Co-Incidence) imaging were done after injection using a dual-head Sopha Medical Vision DST-XL SPECT system with a useful field of view

(UFOV) of 540 mm *400 mm. The biodistribution of the $^{68/67}\text{Ga}$ -labeled protoporphyrin IX-gadolinium complex [$^{68/67}\text{Ga}$]Ga-PP IX-Gd among vital organs of the rodent's body was assessed using high purity germanium (HPGe) Radiation Detector. The percent of initial injected dose per gram of tissue (%ID/g) were recorded.

In-vivo biodistribution studies were performed in mice bearing breast tumor (4T1 mouse mammary tumor cell line) and normal rats (for better visualization). Prepmouseion of breast carcinoma was done according to literature [31], About 200 000–300 000 cells in homogenized mixture were injected subcutaneously into normal mice under sterile conditions. In 3–4 weeks mice with the tumor tissue reaching about 2 cm³ were ready for animal studies.

RESULTS AND DISCUSSION

Synthesis of PP IX-Gd with gallium-67/68

Agondanou et al. have reported the structure and electronic properties of sandwich-like Gd-porphyrin complexes [32]. Other studies have described complexation of the lanthanide (III) cations by porphyrins and confirmed that the lanthanide (III) ions located above the porphyrin plane [33].

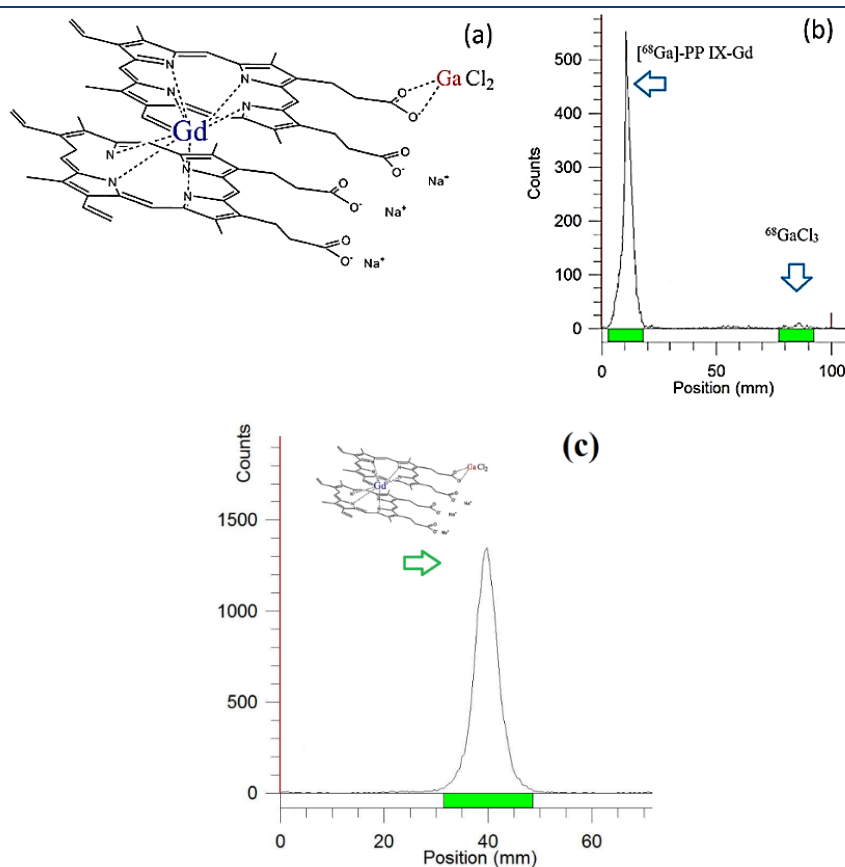


Fig 1. Possible coordination sites for Gd and Ga metals (a). RTLC chromatogram of [^{68}Ga]Ga-PP IX-Gd using DTPA as mobile phase (b) and 10% NH_4OAc (ammonium acetate) /methanol/acetonitrile (1:1:1) as mobile phase (c)

So, Gd (III) ion located above the porphyrin planes in a sandwich form and Gallium-68 complexed by bidentate ligands of propionic acid groups (Figure 1a). Bohle et al.'s study showed that there are inter and intra-molecular interactions between propionic acid groups on porphyrin ring, between neighboring carboxylic acids and between carboxylic acids and metals [9, 10]. So, they can stable metals in the core as well. As shown in Figure 1b, the radiochemical purity of the prepared $[^{68}\text{Ga}]\text{Ga-PP IX-Gd}$ complex was more than 99%. In order to investigate the formation of Ga colloid, preparation of $[^{68}\text{Ga}]\text{Ga-PP IX-Gd}$ was investigated using another RTLC conditions, 10% NH_4OAc (Ammonium Acetate) /methanol/Acetonitrile (1:1:1) as mobile phase on Whatman No. 2 papers as stationary phase. In this condition free Gallium ions remains at the base and complex migrated to higher Rf (0.4). Almost no free Ga ions or colloid was observed [31].

Biodistribution

Among all diagnostic methods for cancer detection, MRI and PET give the most accurate information. So to have a possible PET/MRI agent with ability to use as the photosensitizer, the $[^{68}\text{Ga}]\text{Ga-PP IX-Gd}$ was synthesized and biodistribution in rodents were done. In parallel experiment, $[^{67}\text{Ga}]\text{Ga-PP IX-Gd}$ was also synthesized and planar images were recorded. The biodistribution images of $[^{68}\text{Ga}]\text{Ga-PP IX-Gd}$ in normal rats (Figure 2), $[^{67}\text{Ga}]\text{Ga-PP IX-Gd}$ in normal rats (Figure 3), and $[^{67}\text{Ga}]\text{Ga-PP IX-Gd}$ rats bearing breast tumor (Figure 4) are presented. The difference between the images originates from the difference in imaging methods. In Coincidence mode the distance from head of the camera to animal is about 60 cm (due to the rotation of the heads) and in planar mode the distance is only 12 cm so the resolution in planar mode is better with our device and more details are seen.

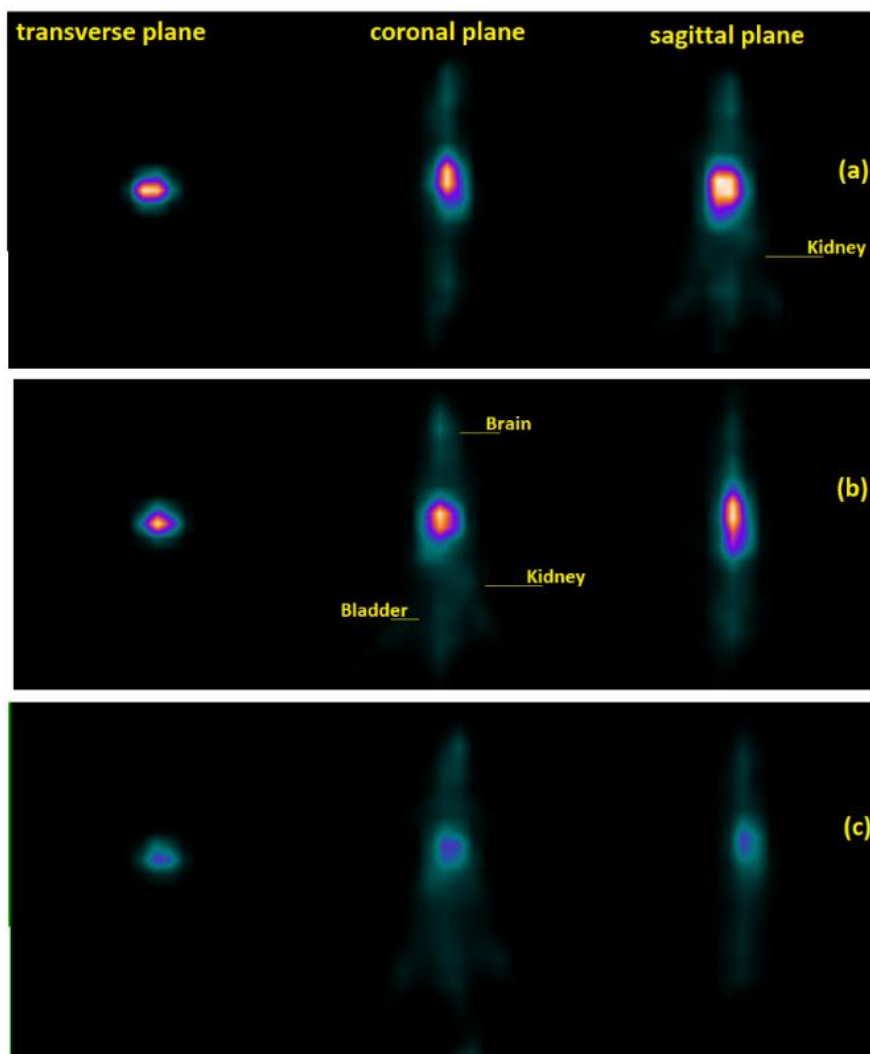


Fig 2. Coincidence imaging of $[^{68}\text{Ga}]\text{Ga-PP IX-Gd}$ in normal rats at 30 min (a), 60 min (b) and 120 min (c) post injection

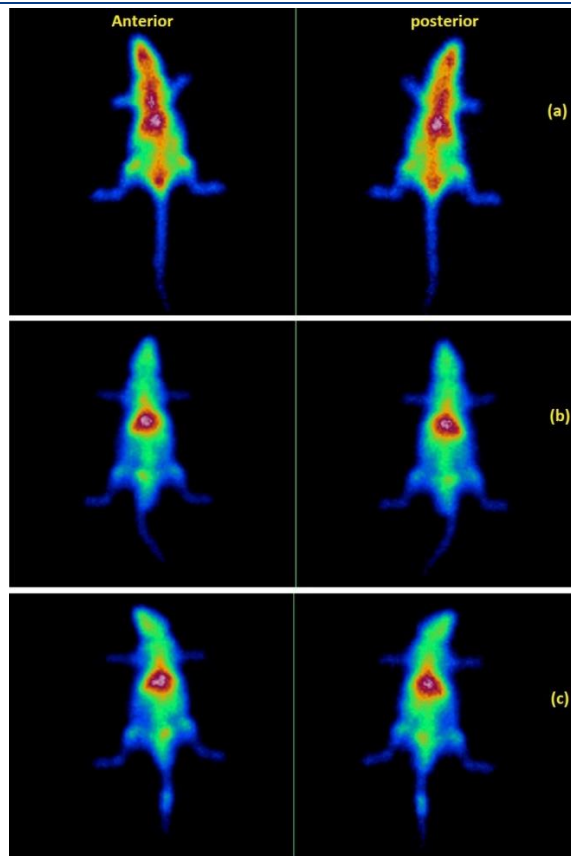


Fig 3. Planar imaging of $[^{67}\text{Ga}]\text{Ga-PP IX-Gd}$ in normal rats at 30 min (a), 60 min (b) and 120 min (c) post injection

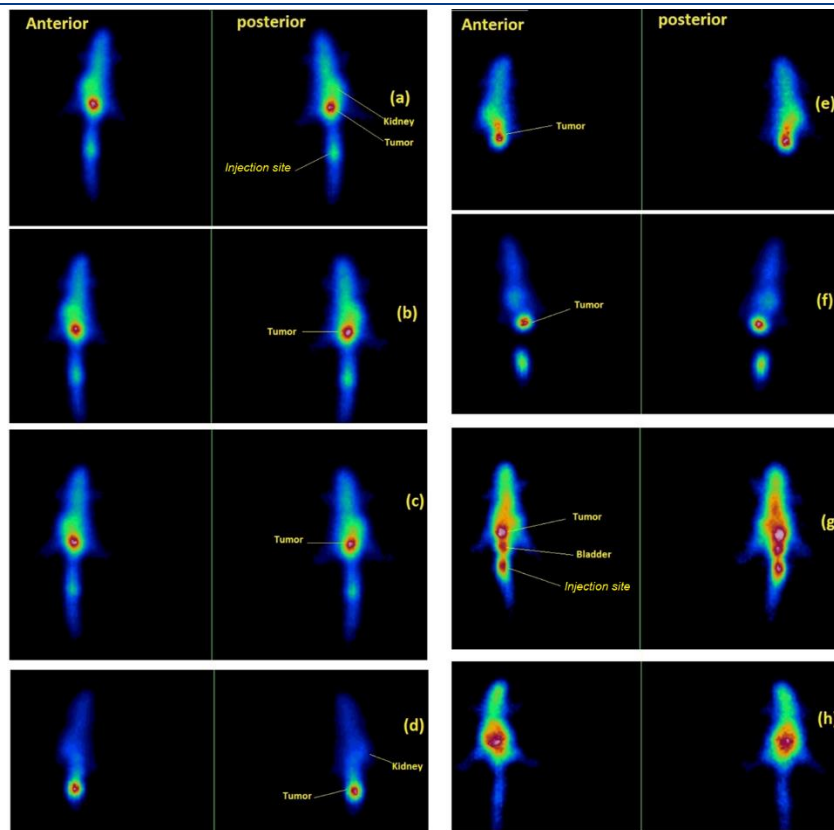


Fig 4. Planar imaging of $[^{67}\text{Ga}]\text{Ga-PP IX-Gd}$ in mice bearing breast tumor at 30 min (a), 45 min (b), 60 min (c), 90 min (d), 120 min (e), 150 min (f), 180 min (g) and 24 h (h) post injection

As shown in Figures 2, 3 and 4, the labeled complex has the significant distribution in the bloodstream at all times after injection and has a suitable distribution in all examined organs and make possibility to detect the tumor in any organ. These labeled compounds even cross the membranes of brain (blood brain barrier) and bone cells and may be suitable for theranostic purposes in these organs. After 4 hours, with the buildup of free gallium metabolite in the liver, its biological distribution in the spleen and gastrointestinal tract is increased. Due to the excretion of gallium radionuclides from kidneys, as well as the very high polarity of proto porphyrin ligand (At the pH 7 the partition coefficients (log P) for $[^{67}\text{Ga}]\text{Ga-PP IX-Gd}$ was -0.48), which is induced by the presence of carboxylic acid groups in the salt form and the presence of gadolinium and gallium ions, these labeled compounds are

mainly excreted from body by the kidneys and their presence in the gut and feces are low. The kidneys also have significant activity at all times after injections, due to the high solubility of the labeled compound in water. Tumor uptake, despite the small size of the lesion, had an upward trend at all times demonstrating high and fast uptake of radiotracer in cancerous tumors. This pattern remains often 24 hours post injection (Figure 4h).

These results are supported by the %ID/g diagram of $[^{68}\text{Ga}]\text{Ga-PP IX-Gd}$ among organs of rats bearing breast tumors which illustrated that the major accumulations of the nanoparticles post-injection were found in the tumor, blood, lung and kidney (Figure 5). The labeled complex showed excellent stability in human albumin serum at 37°C for 4 h, and no measurable amount of free gallium was observed.

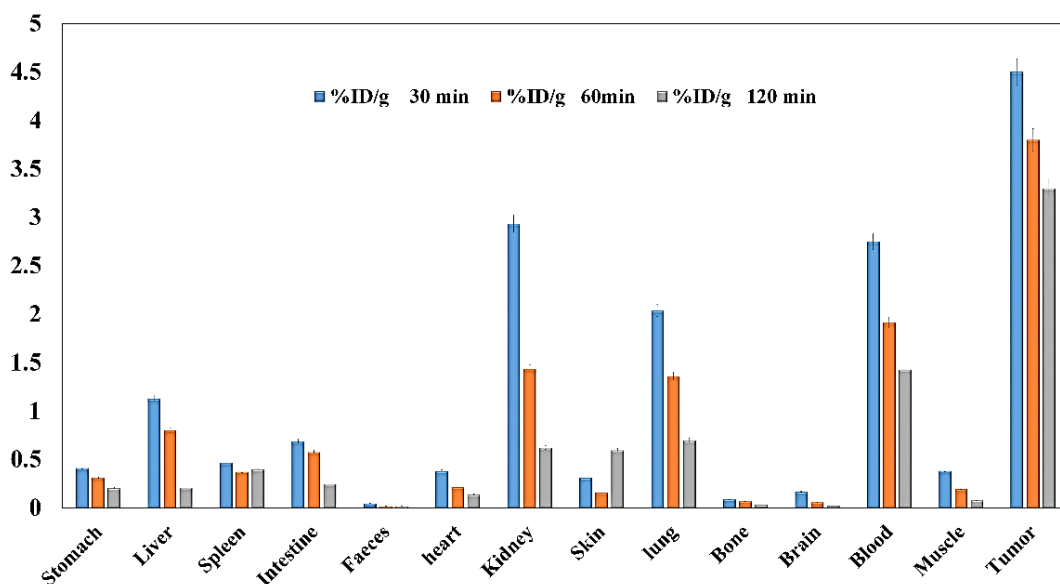


Fig 5. The biodistribution of $[^{68}\text{Ga}]\text{Ga-PP IX-Gd}$ in breast tumor-bearing mice (n=3).

CONCLUSIONS

Novel radiotracers that potentially can be used as SPECT/MRI/PDT or PET/MRI/PDT tri-modality imaging/therapy agents were reported. The prepared $[^{67/68}\text{Ga}]\text{Ga-PP IX-Gd}$ is cleared through renal pathway. Due to the high and fast tumor uptake, lower absorbed dose to patients was achieved. So, $[^{67/68}\text{Ga}]\text{Ga-PP IX-Gd}$ demonstrated attractive characteristics as a promising theranostic agent in PDT-based cancer detection and therapy.

REFERENCES

1. Tong KC, Hu D, Wan PK, Lok CN, Che CM. Anticancer Gold(III) compounds with porphyrin or N-heterocyclic carbene ligands. *Front Chem.* 2020 Nov 6;8:587207.
2. Janas K, Boniewska-Bernacka E, Dyrda G, Słota R. Porphyrin and phthalocyanine photosensitizers designed for targeted photodynamic therapy of colorectal cancer. *Bioorg Med Chem.* 2021 Jan 15;30:115926.
3. Fazaeli Y, Hosseini MA, Shahabinia F, Feizi S. ^{68}Ga -5, 10, 15, 20-Tetrakis (2, 4, 6-trimethoxy phenyl) porphyrin: a novel radio-labeled porphyrin complex for positron emission tomography. *J Radioanal Nucl Chem.* 2019 Apr;320(1):201-7.
4. Ethirajan M, Patel NJ, Pandey RK. Chapter 19: Porphyrin-based multifunctional agents for tumor-imaging and photodynamic therapy (PDT). Kadish KM, Smith KM, Guillard R, editors. *Handbook of porphyrin science volume 4.* Singapore: World Scientific Publishing Company; 2010. p. 249-323.
5. Deda DK, Iglesias BA, Alves E, Araki K, Garcia CRS. Porphyrin derivative nanoformulations for therapy and antiparasitic agents. *Molecules.* 2020 Apr 29;25(9):2080.

6. Yan L, Miller J, Yuan M, Liu JF, Busch TM, Tsourkas A, Cheng Z. Improved photodynamic therapy efficacy of protoporphyrin IX-loaded polymeric micelles using erlotinib pretreatment. *Biomacromolecules*. 2017 Jun 12;18(6):1836-1844.
7. Morales-de-Echegaray AV, Maltais TR, Lin L, Younis W, Kadasala NR, Seleem MN, Wei A. Rapid uptake and photodynamic inactivation of staphylococci by Ga(III)-protoporphyrin IX. *ACS Infect Dis*. 2018 Nov 9;4(11):1564-1573.
8. Juarranz A, Jaén P, Sanz-Rodríguez F, Cuevas J, González S. Photodynamic therapy of cancer. Basic principles and applications. *Clin Transl Oncol*. 2008 Mar;10(3):148-54.
9. Bohle DS, Dodd EL. [Gallium (III) protoporphyrin IX] 2: a soluble diamagnetic model for malaria pigment. *Inorg Chem*. 2012 Apr 16;51(8):4411-3.
10. Bohle DS, Dodd EL, Pinter TB, Stillman MJ. Soluble diamagnetic model for malaria pigment: coordination chemistry of gallium(III)protoporphyrin-IX. *Inorg Chem*. 2012 Oct 15;51(20):10747-61.
11. Pinter TB, Dodd EL, Bohle DS, Stillman MJ. Spectroscopic and theoretical studies of Ga(III)protoporphyrin-IX and its reactions with myoglobin. *Inorg Chem*. 2012 Mar 19;51(6):3743-53.
12. Chang D, Garcia RA, Akers KS, Mende K, Murray CK, Wenke JC, Sanchez CJ. Activity of Gallium meso- and protoporphyrin IX against biofilms of multidrug-resistant acinetobacter baumannii isolates. *Pharmaceuticals (Basel)*. 2016 Mar 17;9(1):16.
13. Stojiljkovic I, Kumar V, Srinivasan N. Non-iron metalloporphyrins: potent antibacterial compounds that exploit haem/Hb uptake systems of pathogenic bacteria. *Mol Microbiol*. 1999 Jan;31(2):429-42.
14. Hijazi S, Visca P, Frangipani E. Gallium-protoporphyrin IX Inhibits *Pseudomonas aeruginosa* growth by targeting cytochromes. *Front Cell Infect Microbiol*. 2017 Jan 26;7:12.
15. Espinosa-Cano E, Palao-Suay R, Aguilar MR, Vázquez B, Román JS. Polymeric nanoparticles for cancer therapy and bioimaging. Gonçalves G, Tobias G, editors. *Nanooncology*. Nanomedicine and Nanotoxicology. 1st ed. Switzerland: Springer Cham; 2018. p. 137-172
16. Zang L, Zhao H, Hua J, Qin F, Zheng Y, Zhang Z, Cao W. Water-soluble gadolinium porphyrin as a multifunctional theranostic agent: Phosphorescence-based oxygen sensing and photosensitivity. *Dyes Pigm*. 2017 Jul 1;142:465-71.
17. Samkoe KS, Gibbs-Strauss SL, Yang HH, Khan Hekmatyar S, Jack Hoopes P, O'Hara JA, Kauppinen RA, Pogue BW. Protoporphyrin IX fluorescence contrast in invasive glioblastomas is linearly correlated with Gd enhanced magnetic resonance image contrast but has higher diagnostic accuracy. *J Biomed Opt*. 2011 Sep;16(9):096008.
18. Guleria M, Das T, Vats K, Amirdhanayagam J, Mathur A, Sarma HD, Dash A. Preparation and evaluation of ^{99m}Tc-labeled porphyrin complexes prepared using PNP and HYNIC cores: studying the effects of core selection on pharmacokinetics and tumor uptake in a mouse model. *Medchemcomm*. 2019 Feb 22;10(4):606-615.
19. Entract GM, Bryden F, Domarkas J, Savoie H, Allott L, Archibald SJ, Cawthorne C, Boyle RW. Development of PDT/PET theranostics: synthesis and biological evaluation of an (18)F-radiolabeled water-soluble porphyrin. *Mol Pharm*. 2015 Dec 7;12(12):4414-23.
20. Hervella P, Dam JH, Thisgaard H, Baun C, Olsen BB, Høilund-Carlsen PF, Needham D. Chelation, formulation, encapsulation, retention, and in vivo biodistribution of hydrophobic nanoparticles labelled with ⁵⁷Co-porphyrin: Oleylamine ensures stable chelation of cobalt in nanoparticles that accumulate in tumors. *J Control Release*. 2018 Dec 10;291:11-25.
21. Fazaeli Y, Feizi S, Jalilian AR, Hejrani A. Grafting of [(64)Cu]-TPPF20 porphyrin complex on Functionalized nano-porous MCM-41 silica as a potential cancer imaging agent. *Appl Radiat Isot*. 2016 Jun;112:13-9.
22. Fazaeli Y, Jalilian AR, Amini MM, Ardaneh K, Rahiminejad A, Bolourinovin F, Moradkhani S, Majdabadi A. Development of a (68)Ga-fluorinated porphyrin complex as a possible PET imaging agent. *Nucl Med Mol Imaging*. 2012 Mar;46(1):20-6.
23. Fazaeli Y, Jalilian AR, Rezaee F, Firouzyar T, Moradkhani S, Bagheri A, Majdabadi A. Development of radiolabeled radachlorin complex as a possible tumor targeting agent. *J Radioanal Nucl Chem*. 2015 Mar;303(3):1695-701.
24. Fazaeli Y, Shanehsazzadeh S, Lahooti A, Feizi S, Jalilian A. Preclinical dosimetric estimation of [111In] 5, 10, 15, 20-tetra phenyl porphyrin complex as a possible imaging/PDT agent. *Radiochim Acta*. 2016 May 28;104(5):327-36.
25. Fazaeli Y, Jalilian AR, Khalaj A. Development of a new radiogallium porphyrin complex as a possible tumor imaging agent. *Int J Nucl Med Res*. 2015 Mar 20;2(1):7-15.
26. Fazaeli Y, Jalilian AR, Feizi S, Shadanpour N. Development of a radiothallium (III) labeled porphyrin complex as a potential imaging agent. *Radiochim Acta*. 2013 Dec 1;101(12):795-800.
27. Eguchi K, Nakamura H, Zhou JR, Jun F, Yokomizo K, Haratake MJ. Hyaluronic acid-zinc protoporphyrin conjugates for photodynamic antitumor therapy. *J Nanomed Nanotechnol*. 2007;8 (2):100400.
28. Zhu B, Liu Q, Wang Y, Wang X, Wang P, Zhang L, Su S. Comparison of accumulation, subcellular location, and sonodynamic cytotoxicity between hematoporphyrin and protoporphyrin IX in L1210 cells. *Chemotherapy*. 2010;56(5):403-10.
29. Lv Y, Zheng J, Zhou Q, Jia L, Wang C, Liu N, Zhao H, Ji H, Li B, Cao W. Antiproliferative and apoptosis-inducing effect of exo-protoporphyrin IX based sonodynamic therapy on human oral squamous cell carcinoma. *Sci Rep*. 2017 Jan 19;7:40967.
30. Tomaszewski MR, Gonzalez IQ, O'Connor JP, Abeyakoon O, Parker GJ, Williams KJ, Gilbert FJ, Bohndiek SE. Oxygen enhanced optoacoustic tomography (OE-OT) reveals vascular dynamics in murine models of prostate cancer. *Theranostics*. 2017 Jul 8;7(11):2900-2913.
31. Vahidfar N, Jalilian AR, Fazaeli Y, Aghanejad A, Bahrami-Samani A, Alirezapour B, Erfani M, Beiki D, Khalaj A. Development of radiolanthanide labeled porphyrin complexes as possible therapeutic agents in breast carcinoma xenografts. *Radiochim Acta*. 2014 Jul 28;102(7):659-68.
32. Agondanou JH, Spyroulias GA, Purans J, Tsikalas G, Souleau C, Coutsolelos AG, Bénazeth S. XAFS study of gadolinium and samarium bisporphyrinate complexes. *Inorg Chem*. 2001 Nov 19;40(24):6088-96.
33. Bulach V, Sguerra F, Hosseini MW. Porphyrin lanthanide complexes for NIR emission. *Coord Chem Rev*. 2012 Aug 1;256(15-16):1468-78.